Electronic Supplementary Material (ESI) for ChemComm.

# Supporting Information

# A new Pu(III) coordination geometry in $(C_5H_5NBr)_2[PuCl_3(H_2O)_5] \cdot 2Cl \cdot 2H_2O$ as obtained via supramolecular assembly in aqueous, high chloride media

Robert G. Surbella III,[1] Lucas C. Ducati,[2] Kristi L. Pellegrini,[3] Bruce K. McNamara,[3] Jochen Autschbach,[4] Jon M. Schwantes,[3] Christopher L. Cahil.[1*]

[1]Department of Chemistry, The George Washington University (800 22nd St NW, Washington, D.C., 20052)
[2]Department of Fundamental Chemistry Institute of Chemistry, University of São Paulo, Av. Prof. Lineu Prestes 748, São Paulo, SP 05508-000, Brazil
[3]Pacific Northwest National Laboratory, 902 Battelle Blvd, Richland, WA 99354.
[4]Department of Chemistry, University at Buffalo, State University of New York, 312 Natural Sciences Complex, Buffalo, New York 14260.

## Table of Contents

## 1. Experimental Notes and Materials

The 4-Bromopyridine · HCl (Aldrich, 99%) was purchased from Sigma-Aldrich and used without further purification.

***Caution!*** $^{239}$Pu ($t_{1/2}$ = 2.4 x $10^4$ y) is hazardous and poses a health risk as it is an α and γ emitting radionuclide. Experiments with this isotope was performed in a facility designed and designated for the handling of transuranic radionuclides. Dispersible solids were handled and manipulated in a negative-pressure radiological glovebox, whereas single-crystals were handled in radiological fume hoods after being coated with Krytox grease or Paratone-N oil.

**Preparation of a $^{239}PuO_2^{2+}$(VI) Stock Solution**

Solid $^{239}$plutonium dioxide dissolved in concentrated nitric acid and < 0.5% by volume hydrofluoric acid over the course of ~7 days. UV-Vis spectroscopy revealed that this emerald green solution contained a mixture of two primary oxidation states, Pu IV and VI. This volume of the solution was reduced to ~0.25 mL and then diluted with 5mL of DI $H_2O$. The solution was heated and stirred while an excess of $NaBrO_{3(s)}$ was slowly added to oxidize the plutonium IV → VI. The volume of the solution was then reduced until moist solids remained, which were then dissolved in concentrated $HCl_{(aq)}$. We note that the addition of HCl in the presence of $NaBrO_{3(aq)}$ produces $Cl_{2(g)}$. This now Pu(VI) chloride solution was boiled to near dryness and rehydrated with concentrated HCl in order to destroy any remaining nitrate, nitrite or bromate species. This process was repeated four times, after which the volume of the gold solution was reduced and cooled. The volume and HCl concentration of the solution was adjusted such that the final stock solution contained 219 mg Pu $mL^{-1}$ (determined by high resolution gamma spectroscopy) in 2mL of 2.5M HCl. The Pu oxidation state was verified VI using UV-VIS spectroscopy (**Figure S1**).

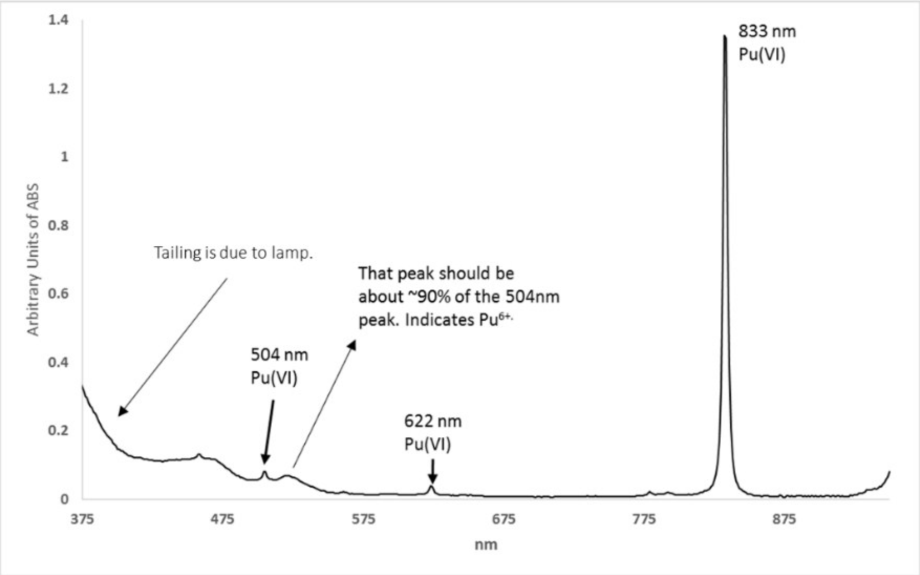

**Figure S1**. The UV-Vis spectrum taken of the $PuO_2^{2+}$ stock solution.

**Synthesis of 1**, $(C_5H_5NBr)_2[PuCl_3(H_2O)_5] \cdot 2Cl \cdot 2H_2O$.

A 1mL aliquot of the Pu stock solution was stirred in a 20mL scintillation vial and gently heated while hydroxylamine ($NH_2OH_{(s)} \cdot HCl$) was added to adjust the oxidation state of the Pu from VI → III. The color of the solution changed from a bright yellow color to brown. The brown color persisted for approximately fifteen seconds, after which the solution became orange and then immediately, a greenish blue. Twelve molar equivalents (based on Pu) of $LiCl_{(s)}$ were added to the solution, which instantly became dark blue in color. A 250µL microliter aliquot of this now Pu(III) chloride solution was added into a small 4mL vial that contained a second solution of 4-bromopyridinium in 100µL of 0.5M HCl. This vial was placed inside of a desiccator – this consisted of a 50mL conical centrifuge tube that was three-quarters filled with Drierite™ desiccant – which was then purged with $Ar_{(g)}$ for three minutes and sealed (**Photo S1**). After two weeks the solution reached dryness and blue transparent crystals of compound **1** were harvested.

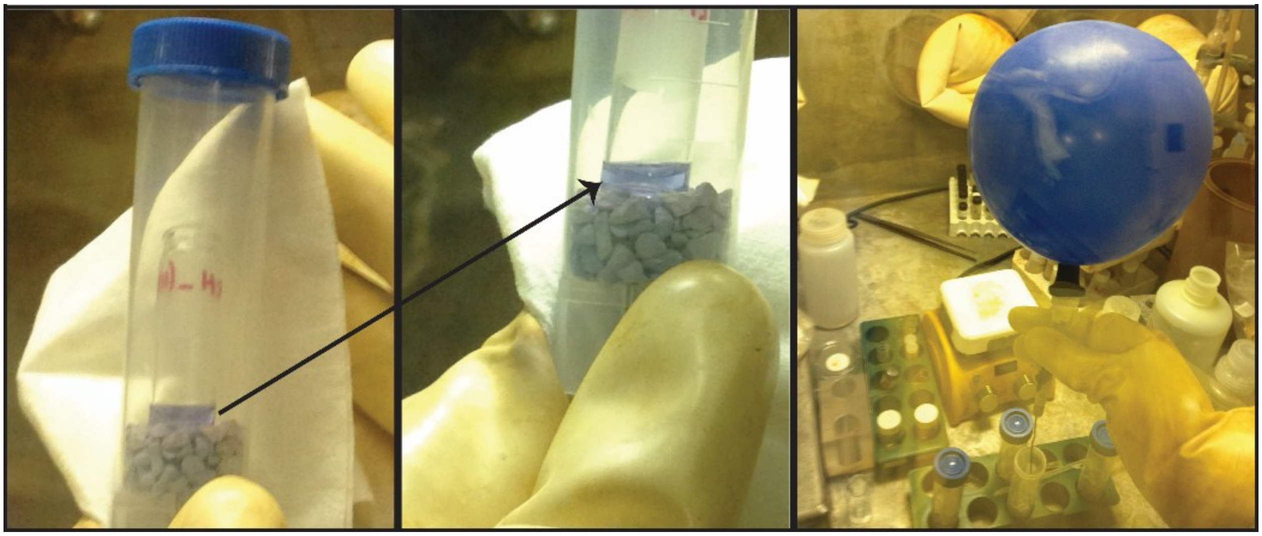

**Photo S1**. The desiccator setup used in the synthesis of **1**. A balloon (right) filled with $Ar_{(g)}$ was affixed to a syringe and used to purge the chamber once inside of the glove box.

**2. Single crystal X-ray diffraction**: **Sample Preparation**

Single crystals of **1** were submerged in Paratone-N oil, selected and cut to the appropriate size for the diffraction experiment. The specimens were coated with either Krytox™ grease or Krazy Glue® and mounted onto the tip of a MiTeGen MicroMount™. A clear heat sealable tube (manufactured by Vention® Medical) made of polyphenylene ether was placed over the MicroMount™ and copper post and affixed with epoxy to ensure containment of the specimen (**Photo S2**).

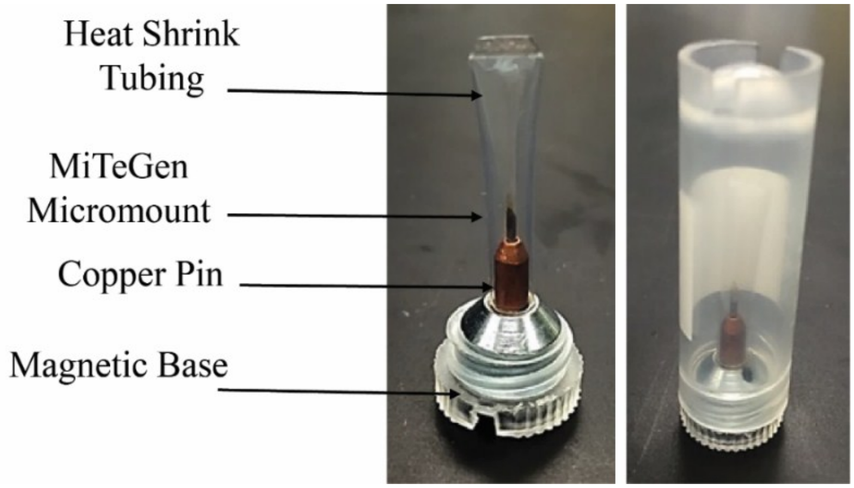

**Photo S2**. A typical crystallographic setup that was used in the data collection of 1. Reprinted with permission from Robert G. Surbella III, Lucas C. Ducati, Kristi L. Pellegrini, Bruce K. McNamara, Jochen Autschbach, Jon M. Schwantes, and Christopher L. Cahill, *Journal of the American Chemical Society*, 2017 139 (31), 10843-10855. Copyright 2017 American Chemical Society.

**Single Crystal X-Ray Diffraction**

Diffraction data were collected using 0.5° φ and ω scans at 296(2)K on a Bruker D8 Venture diffractometer equipped with a Photon 100 CMOS detector and both a standard Mo K-α source and Ag - IμS microfocus source (**Table S1**). The APEX III software suite[1] was used to integrate the data and to apply an adsorption collection (SADABS).[2] The structures were solved using direct methods (SIR92)[3] or *via* charge flipping (SUPERFLIP)[4] methods and refined using SHELXL-14[5] within the WINGX software suite.[6] Materials used for publication were prepared using EnCifer[7] whereas figures of the title compounds were made using CrystalMaker V.9.2.8.[8] The non-hydrogen atoms in **1** were located in difference Fourier maps, modeled and refined anisotropically. The hydrogen atoms on the five coordination water molecules and the two non-coordinated (lattice) waters were able to be located in difference Fourier maps, were modeled, distance (DFIX 0.84, 0.01 and DANG 1.34, 0.02) restrained and refined isotropically. The hydrogen atoms associated with both of the two crystallographically unique 4-bromopyridinium nitrogen atoms were located in difference Fourier maps, modeled, distance restrained (DFIX 0.89, 0.01) and refined isotropically.

**Table S1**. Selected crystallographic data of compound **1**.

| Compound | **1** |
|---|---|
| Formula | $(C_5H_5NBr)_2[PuCl_3(H_2O)_5] \cdot 2Cl \cdot 2H_2O$ |
| Formula mass | 863.38 |
| Temperature (K) | 296(2)K |
| Ag λ (Kα) | 0.56086 |
| Crystal Color and Habit | Blue Prismatic |
| Size | 0.154 x 0.137 x 0.128 |
| Crystal system | Triclinic |
| Space Group | $P\bar{1}$ |
| a (Å) | 8.4714(12) |
| b (Å) | 12.6613(16) |
| c (Å) | 13.5401(19) |
| α (°) | 68.172(4) |
| β (°) | 75.764(4) |
| γ (°) | 71.127(4) |
| Volume (Å$^3$) | 1262.6(3) |
| $D_{calc}$ (Mg m$^{-3}$) | 2.271 |
| Z | 2 |
| μ (mm$^{-1}$) | 5.599 |
| No. of reflections measured | 75969 |
| No. of independent reflections | 6974 |
| $R_{int}$ | 0.0278 |
| Final $R_1$ values ($I > 2\sigma(I)$) | 0.0234 |
| Final $wR_2$ ($F^2$) values ($I > 2\sigma(I)$) | 0.0599 |
| Goodness of fit on $F^2$ | 1.168 |
| CCDC number | 1565318 |

### 3. Additional Figures of $(C_5H_5NBr)_2[PuCl_3(H_2O)_5] \cdot 2Cl \cdot 2H_2O$

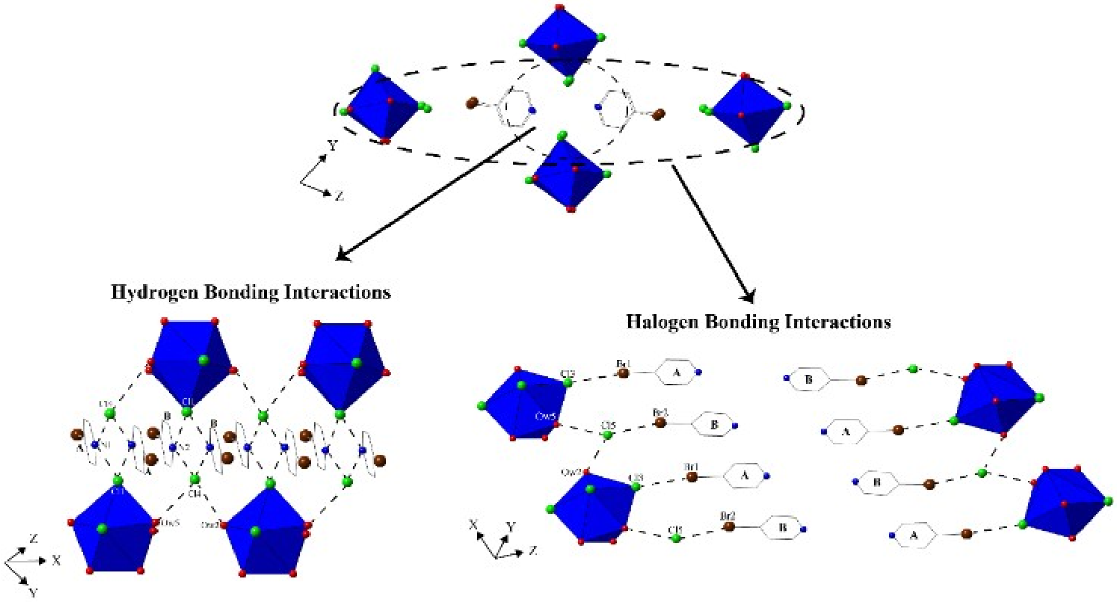

**Figure S2**. Top: A portion of **1** highlighting the positioning of the 4-BrPyH cations relative to the $[PuCl_3(H_2O)_5]$ tectons. Bottom: The 4-BrPyH cations form hydrogen (left) and halogen bonds (right) that link the $[PuCl_3(H_2O)_5]$ tectons together. In addition to the hydrogen atoms, a number of chloride anions, water molecules and $[PuCl_3(H_2O)_5]$ tectons have been omitted for clarity.

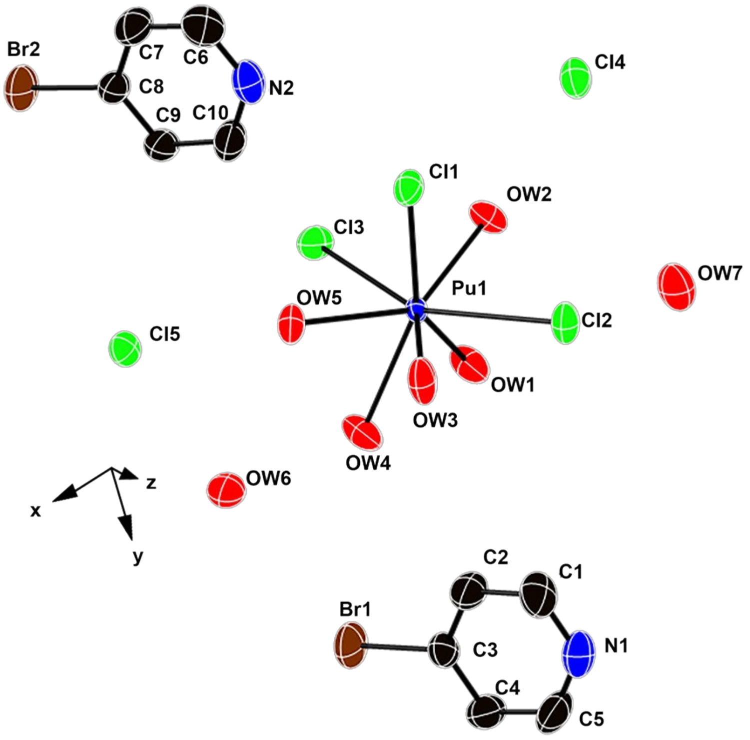

**Figure S3**. A thermal ellipsoidal representation of the asymmetric unit of **1**. Thermal ellipsoids are drawn at the 50% probability level.

## 4. Selected interaction distances

**Table S2**. Selected bond distances and angles within the [$PuCl_3(H_2O)_5$] tecton in **1**.

| **Bond** | **Distance (Å)** |
|---|---|
| Pu – Cl1 | 2.7641(10) |
| Pu – Cl2 | 2.8154(12) |
| Pu – Cl3 | 2.8333(12) |
| Pu – Ow1 | 2.526(4) |
| Pu – Ow2 | 2.489(4) |
| Pu – Ow3 | 2.513(3) |
| Pu – Ow4 | 2.501(4) |
| Pu – Ow5 | 2.485(3) |

**Table S3**. Selected hydrogen and halogen bonding interaction distances and angles featured in **1**.

| **Interaction** | **Distance (Å)** | **Angle** | **Interaction** | **Distance (Å)** | **Angle** |
|---|---|---|---|---|---|
| Ow$_1$-Hw$_1$···Cl$_5$* | 3.311(3) | 156.4° | Ow$_6$-Hw$_{11}$···Cl$_2$ | 3.067(3) | 172.1° |
| Ow$_1$-Hw$_2$···O$_{w6}$* | 2.938(4) | 167.1° | Ow$_6$-Hw$_{12}$···Cl$_5$ | 3.178(3) | 174.7° |
| Ow$_2$-Hw$_3$···Cl$_5$* | 3.172(3) | 157.4° | Ow$_7$-Hw$_{13}$···Cl$_3$ | 3.161(3) | 131.5° |
| Ow$_2$-Hw$_4$···Cl$_4$* | 3.104(3) | 162.3° | Ow$_7$-Hw$_{14}$···Ow$_6$* | 2.903(5) | 155.9° |
| Ow$_3$-Hw$_5$···Cl$_4$* | 3.109(3) | 119.0° | N$_1$-H$_{n1}$···Cl$_1$ | 3.235(4) | 125.5° |
| Ow$_3$-Hw$_6$···Cl$_5$* | 3.222(3) | 157.2° | N$_1$-H$_{n1}$···Cl$_4$* | 3.355(4) | 137.5° |
| Ow$_4$-Hw$_7$···O$_{w6}$* | 2.844(4) | 171.1° | C$_3$-Br$_1$···Cl$_2$ | 3.4413(13) | 171.78(15)° |
| Ow$_4$-Hw$_8$···Cl$_5$* | 3.134(4) | 168.9° | N$_2$-H$_{n2}$···Cl$_1$ | 3.495(4) | 120.4° |
| Ow$_5$-Hw$_9$···Cl$_3$ | 3.208(3) | 162.5° | N$_2$-H$_{n2}$···Cl$_4$* | 3.088(4) | 149.0° |
| Ow$_5$-Hw$_{10}$···Ow$_7$* | 2.697(5) | 153.5° | C$_8$-Br$_2$···Cl$_5$* | 3.2946(12) | 162.91(15)° |

*Denotes an interaction with a non-coordinated lattice water or chloride anion.

## 5. Electrostatic Potential Calculation Details

The atomic coordinates of the [$PuCl_3(H_2O)_5$] tecton were obtained from the crystallographic data. The electrostatic potential (ESP) was calculated with Kohn-Sham (KS) DFT using Gaussian 09 (rev. D.01)[9] within the GaussView5.0 interface.[10] The KS calculations were performed using the M06-2X[11] functional and the following basis sets: Pu - 60MWB-SEG + ECP-60MWB,[12-14] Cl, and Br - def2-TZVP; C, N, and O - def2-TZVP; and H - def2-SVP.[15]

The electrostatic potential, $V(r)$, of a molecule at a point $r$ is described by Equation 1, where: $Z_A$ is the charge on a nucleus $A$, located at $R_A$, and $\rho(r)$ is the electron density of the molecule.

$$V(r) = \sum_A \frac{Z_A}{|R_A - r|} - \int \frac{\rho(r')}{|r' - r|} dV' \qquad \text{Eq. 1}$$

The ESP is given here in atomic units (au) and refers to a fictitious positive probe charge of 1 au placed at position ***r***. A negative/positive potential indicates an electron-rich/deficient region. Information about the response of the molecule to the presence of the probe charge is not contained in the ESP and its graphical visualizations. In order to deduce chemically relevant information, the ESP is usually mapped onto a van der Waals surface or an iso-density surface. In this work, we generated electron density iso-surfaces at 0.001 au (electrons per bohr$^3$), based upon a recommendation by Bader *et al.*[16] as the iso-surface encompasses most of the integrated electron density and is considered to occur at distances from the nuclei that are most relevant for evaluating non-covalent interactions.[17,18]

## 6. References

(1) *Apex III*, Bruker AXS Inc.: Madison, Wisconsin, USA, 2015.

(2) Krause, L.; Herbst-Irmer, R.; Sheldrick, G. M.; Stalke, D. *J. Appl. Crystallogr.* **2015**, *48*, 3.

(3) Altomare, A.; Cascarano, G.; Giacovazzo, C.; Guagliardi, A. *J. Appl. Crystallogr.* **1994**, *27*, 435.

(4) Palatinus, L.; Chapuis, G. *J. Appl. Crystallogr.* **2007**, *40*, 786.

(5) Sheldrick, G. M. *Acta Crystallogr. A* **2008**, *64*, 112.

(6) Farrugia, L. *J. Appl. Crystallogr.* **2012**, *45*, 849.

(7) Allen, F. H.; Johnson, O.; Shields, G. P.; Smith, B. R.; Towler, M. *J. Appl. Crystallogr.* **2004**, *37*, 335.

(8) Palmer, D.; Palmer, S. *CrystalMaker V9.2.7* **2016**.

(9) *Gaussian 09, Revision D.01,* M. J. Frisch, G. W. Trucks, H. B. Schlegel, G. E. Scuseria, M. A. Robb, J. R. Cheeseman, G. Scalmani, V. Barone, G. A. Petersson, H. Nakatsuji, X. Li, M. Caricato, A. Marenich, J. Bloino, B. G. Janesko, R. Gomperts, B. Mennucci, H. P. Hratchian, J. V. Ortiz, A. F. Izmaylov, J. L. Sonnenberg, D. Williams-Young, F. Ding, F. Lipparini, F. Egidi, J. Goings, B. Peng, A. Petrone, T. Henderson, D. Ranasinghe, V. G. Zakrzewski, J. Gao, N. Rega, G. Zheng, W. Liang, M. Hada, M. Ehara, K. Toyota, R. Fukuda, J. Hasegawa, M. Ishida, T. Nakajima, Y. Honda, O. Kitao, H. Nakai, T. Vreven, K. Throssell, J. A. Montgomery, Jr., J. E. Peralta, F. Ogliaro, M. Bearpark, J. J. Heyd, E. Brothers, K. N. Kudin, V. N. Staroverov, T. Keith, R. Kobayashi, J. Normand, K. Raghavachari, A. Rendell, J. C. Burant, S. S. Iyengar, J. Tomasi, M. Cossi, J. M. Millam, M. Klene, C. Adamo, R. Cammi, J. W. Ochterski, R. L. Martin, K. Morokuma, O. Farkas, J. B. Foresman, and D. J. Fox: Gaussian, Inc, Wallingford, CT, 2009.

(10) Dennington, R.; Keith, T.; Millam, J.; Semichem Inc. : Shawnee Mission, KS, 2009.

(11) Zhao, Y.; Truhlar, D. G. *Theor. Chem. Acc.* **2008**, *120*, 215.

(12) Küchle, W.; Dolg, M.; Stoll, H.; Preuss, H. *J. Chem. Phys.* **1994**, *100*, 7535.

(13) Cao, X.; Dolg, M.; Stoll, H. *J. Chem. Phys.* **2003**, *118*, 487.

(14) Cao, X.; Dolg, M. *Comp. Theor. Chem.* **2004**, *673*, 203.

(15) Weigend, F.; Ahlrichs, R. *Phys. Chem. Chem. Phys.* **2005**, *7*, 3297.

(16) Bader, R. F. W.; Carroll, M. T.; Cheeseman, J. R.; Chang, C. *J. Am. Chem. Soc.* **1987**, *109*, 7968.

(17) Murray, J. S.; Politzer, P. *Croat. Chem. Acta* **2009**, *82*, 267.

(18) Clark, T.; Hennemann, M.; Murray, J. S.; Politzer, P. *J. Mol. Model.* **2007**, *13*, 291.